(FWHM) of 0·8 nm was found. Assuming a triangular grating, these values correspond to an effective index modulation of $3{\cdot}3 \times 10^{-3}$, which in turn can be related to an etching depth of 100 nm for the grating. This agrees with values measured from SEM photographs.

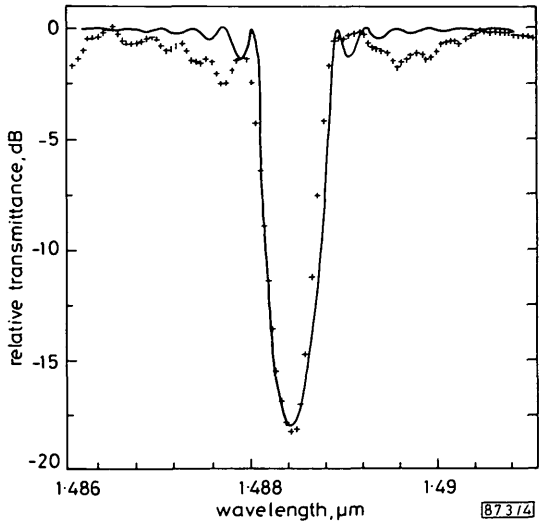

Fig. 4 *Filter response of channel 1 for TE polarisation*
Points: experimental data; line: coupled mode theory

Measurements of the propagation losses of the guides were made on a sample without Bragg gratings. They indicated losses of the straight sections of about 6 dB/cm and additional bending and branching losses of the Y-branch of 1 dB.

Conclusions: The authors have reported on the first demonstration of an InGaAsP Y-branch grating demultiplexer. This device is suitable for further integration with photodiodes. For TE polarisation, a crosstalk attenuation of more than 18 dB and a channel spacing of 13·5 nm was achieved.

Acknowledgment: The authors wish to thank V. Kulich for technical assistance and G. Gorges for the SEM photograph. This work has been supported by the Federal Ministry for Research & Technology of the Federal Republic of Germany under grant no. TK 0273/3. The authors alone are responsible for the content.

C. CREMER
G. HEISE
R. MÄRZ
H. RIECHERT
M. SCHIENLE

Research Laboratories of Siemens AG
Otto-Hahn-Ring 6
D-8000 München 83, W. Germany

2nd February 1987

References

1 WINZER, G.: 'Wavelength multiplexing components—a review of single-mode devices and their applications', *IEEE J. Lightwave Technol.*, 1984, **LT-2**, pp. 369–378
2 SCHMIDT, R. V., FLANDERS, D. C., SHANK, C. V., and STANLEY, R. D.: 'Narrow-band grating filters for thin-film optical waveguides', *Appl. Phys. Lett.*, 1974, **25**, pp. 651–652
3 ALFERNESS, R. C., JOYNER, C. H., DIVINO, M. D., and BUHL, L. L.: 'InGaAsP/InP waveguide grating filters for $\lambda = 1{\cdot}5\,\mu$m', *ibid.*, 1984, **45**, pp. 1278–1280
4 YARIV, A.: 'Coupled-wave theory for guided wave optics', *IEEE J. Quantum Electron.*, 1975, **QE-9**, pp. 919–933

SECOND-HARMONIC GENERATION IN AN OPTICAL FIBRE BY SELF-WRITTEN $\chi^{(2)}$ GRATING

Indexing terms: Optical fibres, Harmonic generation

A mechanism for phase-matched generation of second-harmonic (SH) light in an optical fibre has been experimentally and theoretically studied. A weak non-phase-matched SH signal, created via the quadrupole polarisation, initiates the self-writing of an axially periodic pattern of colour centres which is postulated to lead to the growth of a $\chi^{(2)}$ grating. The grating (at the phase-match period) gives rise to SH generation at efficiencies of 0·5%. The spectral bandwidth of this $\chi^{(2)}$ grating is 0·24 nm.

Introduction: Second-harmonic generation (SHG) by an electric-dipole process is normally forbidden in a fused-silica fibre for two reasons: (i) silica possesses a centrosymmetric structure and (ii) it is difficult to achieve a phase-matching condition. Despite this, however, SHG of an Nd : YAG laser operating at 1·06 μm has been recently reported[1] with efficiencies over 1%. The second-harmonic (SH) signal was observed to grow exponentially over a period of 8 h. We report here similar efficiencies for SHG, together with experimental evidence that the effect is due to the existence of a spatially periodic 2nd-order nonlinear susceptibility $\chi^{(2)}$ in the fibre. Our hypotheses and experimental results are further supported by a coupled-wave theory in which it is shown that the phase-matching condition can be satisfied by the $\chi^{(2)}$ grating vector.

Physical mechanism: In silica optical fibres very weak SHG occurs at high pump intensities owing to a nonlinear electric quadrupole susceptibility.[2] For a pump wavelength λ_p of 1·064 μm the coherence length Λ_c between the pump and the SH at 532 nm is approximately 30 μm as a result of both material and waveguide dispersion. This gives rise to a 30 μm periodic intensity pattern of SHG (green) light along the fibre as energy is interchanged between pump and SH generated light.

In certain fibres with SiO_2 cores doped with GeO_2 and P_2O_5, semipermanent colour centres can be created by short-wavelength radiation.[3] These are known to form dipole centres which we postulate give rise to enhanced second-order nonlinear susceptibility. If this is the case, phase matching will be automatically achieved because the colour centres which enhance $\chi^{(2)}$ will be written periodically into the fibre at spatial locations where the green light intensity is highest, i.e. where the pump and second-harmonic signal are in phase. At points where the pump and SH are out of phase few colour centres are generated. This results in reduced $\chi^{(2)}$ and hence no destructive interference between existing generated green light and the second-order polarisation due to the nonlinear process.

The formation of colour centres is slow at 532 nm and increases rapidly with intensity. Thus it takes time to create the spatial grating in $\chi^{(2)}$ within the fibre, and this gives rise to the observed rapid growth of SH light.

Coupled-wave analysis: We assume that the self-written $\chi^{(2)}$ is sinusoidally modulated with distance x along the fibre at a period equal to the coherence length Λ_c of the SH polarisation at $\lambda_p = \lambda_{po}$ (the writing wavelength). This gives an electric polarisation

$$P = \varepsilon_0(E_p \chi_p + E_s \chi_s) + \varepsilon_0 \chi^{(2)}[1 + M^{(2)} \cos Kx]E^2 \quad (1)$$

where

$$E = E_p + E_s \quad (2)$$

$K = 2\pi/\Lambda_c$, $M^{(2)}$ is the modulation strength of the grating, χ_p and χ_s are the susceptibilities at the pump (ω_p) and SH (ω_s) frequencies, and E_p and E_s are the corresponding electric fields. As we shall show, this $\chi^{(2)}$ grating automatically ensures phase-matching (at $\lambda_p = \lambda_{po}$) between E_p and E_s. The resulting total electric field is

$$E = A_p \exp(-j[k_p x - \omega_p t]) + A_{-ls} \exp(-j[k_s x - \omega_s t]) + \text{constant} \quad (3)$$

For exact phase-matching between E_p and E_s, $K = 2k_p - k_s$, with $k_p = (2\pi/\lambda_p)N_p$ and $k_s = (2\pi/\lambda_s)N_s$, where λ_p, λ_s are vacuum wavelengths and N_p, N_s are the effective refractive

indices. Putting eqn. 3 into the wave equation with P as polarisation, neglecting second-order spatial derivations of the amplitudes A_i and placing the coefficients of terms with identical phase velocities to zero, leads to the following pair of equations:

$$\left.\begin{aligned} \frac{da_p}{dx} + j\gamma a_p^* a_s = 0 \\ \frac{da_s}{dx} + j2\gamma^* a_p^2 = 0 \end{aligned}\right\} \quad (4)$$

$$\gamma = \kappa^{(2)}\{\exp[-jv^{(2)}x] + 0{\cdot}5M^{(2)}\exp[jv_g x]\} \quad (5)$$

where

$$\left.\begin{aligned} a_i &= A_i/A_p(0) \\ v^{(2)} &= k_s - 2k_p \\ v_g &= (\Delta\lambda_p/\lambda_{po})n^{(2)} \\ \kappa^{(2)} &= \frac{A_p(0)k_p\chi^{(2)}}{N_p^2} \end{aligned}\right\} \quad (6)$$

are, respectively, the field amplitudes normalised to the initial pump amplitude $A_p(0)$, the SH dephasing parameter, the grating dephasing parameter and the SH coupling constant. Power conversion is obeyed by solutions of eqns. 4 since one can show that $|a_s|^2 + 2|a_p|^2$ is constant. The key to the very large enhancement in SHG produced by a $\chi^{(2)}$ grating lies in eqn. 5. The first part of γ yields the usual highly dephased (and hence very inefficient) SH coupling for constant $\chi^{(2)}$. The second part contributes SH coupling that is exactly phase-matched if $v_g = 0$, i.e. if $\lambda_p = \lambda_{po}$. Neglecting therefore the first term in γ, and solving first for zero pump depletion ($da_p/dx = 0$):

$$|a_s|^2 \quad (x \leq L) = \{\kappa^{(2)}M^{(2)}x\}^2 \operatorname{sinc}^2\{v_g x/2\} \quad (7)$$

where L is the total grating length. Hence for conversion efficiencies of less than about 5% the spectral bandwidth $\Delta\lambda_{p(1/2)}$ of the SHG process is

$$\Delta\lambda_{p(1/2)} = 4\sqrt{(2)}\lambda_{po}/v^{(2)}L \quad (8)$$

In the presence of pump depletion and for $v_g = 0$ an exact solution exists:

$$|a_s|^2 \quad (x \leq L) = 2\tanh^2\{\kappa^{(2)}M^{(2)}x/\sqrt{2}\} \quad (9)$$

Thus peak conversion efficiency to the SH is approximately quadratic with x for $\kappa^{(2)}M^{(2)}x \ll 1$. However, much more significant is that the $\chi^{(2)}$ grating potentially yields efficiencies approaching 100% for large enough L, as is commensurate with phase-matching.

Experiment: Mode-locked, Q-switched pulses of <100 ps duration and peak powers of 10 kW from an Nd : YAG laser at 1·064 μm were launched into a variety of single-mode fibres. Very weak second- and third-harmonic generation was observed in several. To date, however, growth in SHG has only been observed in a silica fibre with the core and cladding doped with $<1\%$ P_2O_5 and the core doped with 15% GeO_2. The SH signal grew with time from 100 pW to 50 W over a period of 10 h.

To confirm the establishment of a $\chi^{(2)}$ grating, the wavelength dependence of SHG was measured. Pulses from a tunable Raman-shifted dye laser of 6 ns duration and peak powers of 1 kW were launched into a fibre with a previously burnt-in $\chi^{(2)}$ grating. The pump was tuned over 4 nm, giving a measured $\Delta\lambda_{p(1/2)}$ of 0·24 nm for the SH signal, as shown by the experimental points in Fig. 1. The same behaviour resulted when the fibre was pumped from the other end. A best fit of eqn. 4 to the experimental data occurs at an effective grating length L of 12 cm, with $v^{(2)} = 2\pi/\Lambda_c = 0{\cdot}207\,\mu m^{-1}$. Side-scatter measurements nearer the input end of the grating region gave significantly broader linewidths, as one would expect from eqn. 8.

Fig. 1 shows that the largest discrepancies between experiment and theory occur in the sidelobes. This is likely to be linked to nonuniformities in grating phase (and to a lesser extent $M^{(2)}$ and $\chi^{(2)}$) along the fibre. Such variations are an inevitable consequence of the self-writing process, and a more elaborate theory is at present being developed to deal with these effects. Their presence is confirmed in Fig. 2, where a side-scatter measurement of the SH intensity is plotted as a function of distance from the fibre end. The pump light was launched from the opposite end of the fibre. It can be appreciated that about 90% of the conversion occurs in the last 15 cm, which agrees quite well with our best-fit value of 12 cm.

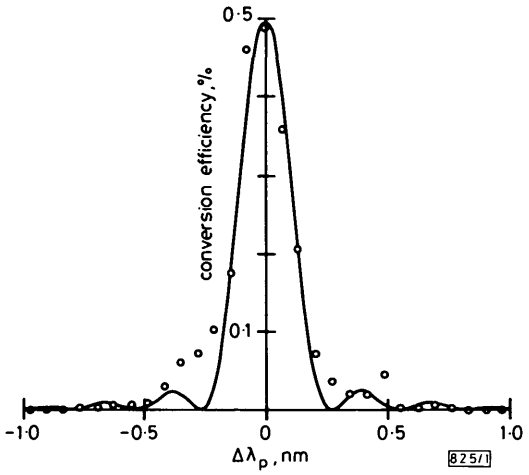

Fig. 1 *Wavelength dependence of SH conversion for deviations of pump wavelength from 1·064 μm*

Circles are experimental points and solid curve a best theoretical fit

A variety of different phenomena are likely to contribute to these axial nonuniformities in grating properties, such as the manifestly nonlinear x-dependence of the growing SH signal, group velocity walk-off between pump and SH, and pump depletion due to stimulated Raman or Brillouin scattering. The efficiency of SHG—as distinct from the writing process—will level off at very high pump powers owing to competing nonlinear processes such as the two just mentioned.

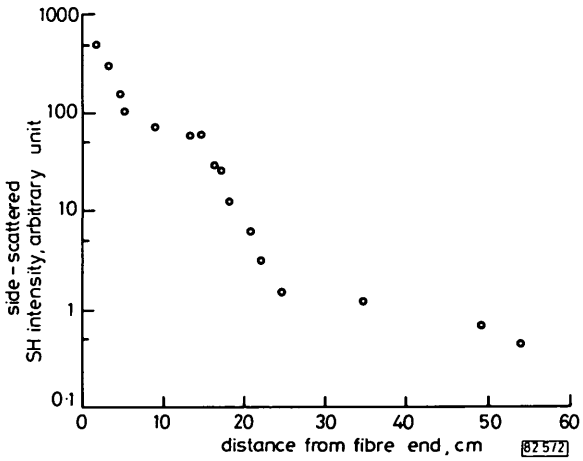

Fig. 2 *Measured side-scattered SH intensity as a function of distance from fibre end*

While the $\chi^{(2)}$ grating was written with pump light launched from the left, this measurement was made with pump light launched from the opposite (RH) end

Finally, an estimate of the product $\chi^{(2)}M^{(2)}$, the modulation depth of $\chi^{(2)}$, can be made if we take our result of 0·5% conversion efficiency at $\lambda_p = \lambda_{po}$ and compare it with the peak value given by eqn. 7. For the fibre spot-size diameter of 5 μm, $\lambda_{po} = 1{\cdot}064\,\mu m$ and a peak pulse power of 10 kW, 0·5% conversion occurs if $\chi^{(2)}M^{(2)} = 2{\cdot}75 \times 10^{-16}$ m/V. From eqn. 9, 60% conversion would be achieved if a grating of this strength were uniform over 1·7 m of fibre.

Conclusions: We have confirmed experimentally that 1% efficient second-harmonic generation is possible in an optical fibre. We postulate that the mechanism is due to the gener-

ation of a grating of colour centres which enhance the second-order susceptibility. The grating period is matched to the coherence length between pump and SH waves. Confirmation of the grating model is provided by our measurements of the operating bandwidth as 0·24 nm.

Acknowledgments: The authors are grateful to R. McGowan and R. Bailey for supplying the optical fibre. M. C. Farries is supported by the UK SERC under the JOERS scheme. D. N. Payne receives a Readership from Pirelli General.

M. C. FARRIES
P. ST. J. RUSSELL
M. E. FERMANN
D. N. PAYNE

Optical Fibre Group
Department of Electronics & Computer Science
University of Southampton
Southampton SO9 5NH, United Kingdom

20th January 1987

References

1 OSTERBERG, U., and MARGULIS, W.: 'Dye laser pumped by Nd : YAG laser pulses frequency doubled in a glass optical fibre', *Opt. Lett.*, 1986, **11**, pp. 516–518
2 BETHUME, D. S.: 'Quadrupole second-harmonic generation for a focused beam of arbitrary transverse structure and polarisation', *ibid.*, 1981, **6**, pp. 287–289
3 GREAVES, G. N.: 'Intrinsic and modified defect states in silica', *J. Non-Cryst. Solids*, 1979, **32**, pp. 295–311

INDIUM PHOSPHIDE AND QUATERNARY DOPING SUPERLATTICES GROWN BY LIQUID-PHASE EPITAXY

Indexing term: Semiconductor devices and materials

Stacks containing from 20 to 100 alternating *n*- and *p*-layers, each less than 100 nm thick, have been produced by liquid-phase epitaxy in both InP and in the quaternary alloy $In_{1-x}Ga_xAs_yP_{1-y}$. Increasing the excitation intensity shifts the photoluminescence (PL) towards shorter wavelengths by the expected magnitude. Hetero-*nipi* quaternary structures displaying two PL peaks have also been grown. The relative intensities of the two peaks depend strongly on the excitation intensity.

Doping superlattices are semiconductor structures comprising multiple layers alternately doped with acceptors and donors. The theory of such structures and their realisation in GaAs by MBE growth have been described by Döhler and Ploog.[1–3] Doping superlattices in GaAs have also been produced by LPE[4] and by MOCVD.[5] Analogous InP structures have been produced by hydride VPE[6] and by MOCVD.[7] All these structures display a photoluminescence peak at a longer wavelength than that corresponding to the simple direct gap transition, with a decrease in the wavelength as the excitation intensity is increased. König and Jorke[8] used LPE to produce periodic doping variations in $In_{0.53}Ga_{0.47}As$ on InP, but the thicknesses and dopant concentrations were not appropriate for doping superlattice characteristics.

We now report the growth of InP and lattice-matched quaternary *npnp* superlattices by LPE at 600°C in an automatically operated furnace incorporating a graphite boat with a linear slider. Layers as thin as 50 nm were grown alternately from two solutions with identical compositions apart from doping with Te or Zn at concentrations giving n or $p = 1 \times 10^{18}\,cm^{-3}$ in thick layers.

Photoluminescence spectra were obtained using 514 nm argon laser radiation at powers from about 1 mW to 1 W focused and unfocused. The *npnp* samples were held at 80 K in a flow cryostat; the PL was analysed using a 1 m spectrometer and an ADC cooled Ge PIN detector. The spectra shown in Fig. 1 demonstrate the peak shift with excitation power which is characteristic of a doping superlattice. The peak wavelength is plotted against the logarithm of excitation power in Fig. 2 (peaks A and B). It shows the expected linear behaviour, except at very high and very low excitation power densities.

The slope of 30 meV/decade obtained here for the quaternary superlattice is similar to that previously reported[4–9] for other semiconductor doping superlattices with doping in the

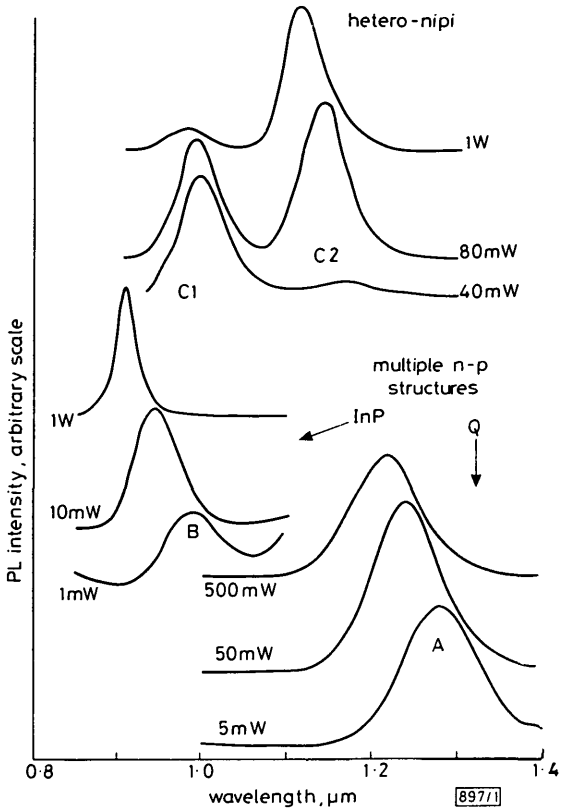

Fig. 1 *Luminescence spectra of quaternary (Q, peak A) and InP doping superlattices (peak B), and of a quaternary hetero-nipi structure showing peaks C1 and C2*

Excitation powers are marked on the curves. Spectra are offset vertically for clarity

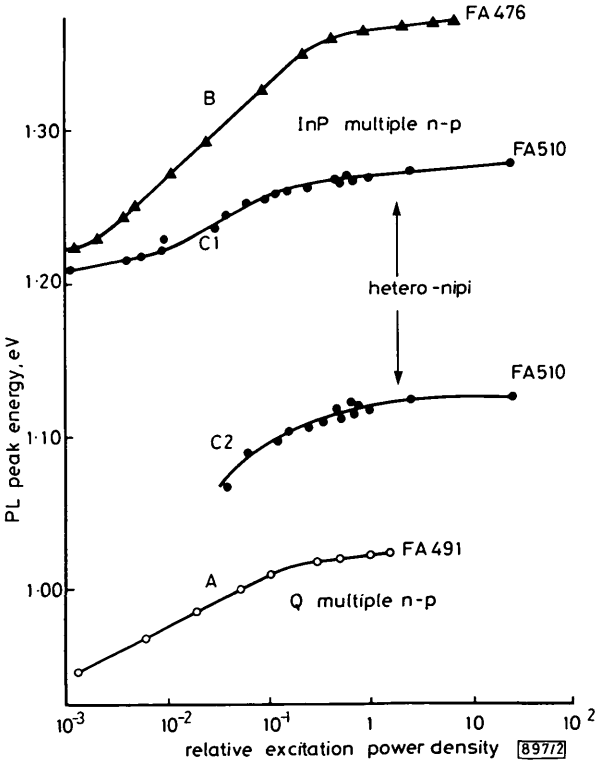

Fig. 2 *Excitation power density dependence of peaks seen in spectra of Fig. 1*

Since varying degrees of focus are used for excitation laser beam, power density is not standardised and curves are not directly comparable on this axis